Monolithic 9 GHz passively mode locked quantum dot lasers directly grown on on-axis (001) Si

Songtao Liu, Justin C. Norman, Daehwan Jung, MJ Kennedy, Arthur C. Gossard, and John E. Bowers

Citation: Appl. Phys. Lett. **113**, 041108 (2018); doi: 10.1063/1.5043200
View online: https://doi.org/10.1063/1.5043200
View Table of Contents: http://aip.scitation.org/toc/apl/113/4
Published by the American Institute of Physics

Monolithic 9 GHz passively mode locked quantum dot lasers directly grown on on-axis (001) Si

Songtao Liu,[1,a),b)] Justin C. Norman,[2,a)] Daehwan Jung,[3] MJ Kennedy,[1] Arthur C. Gossard,[1,2,3] and John E. Bowers[1,2,3]
[1]*Department of Electrical and Computer Engineering, University of California, Santa Barbara, California 93106, USA*
[2]*Materials Department, University of California, Santa Barbara, California 93106, USA*
[3]*Institute for Energy Efficiency, University of California, Santa Barbara, California 93106, USA*

(Received 6 June 2018; accepted 15 July 2018; published online 27 July 2018)

Optical frequency comb direct generation on silicon by mode locked lasers (MLLs) is promising as it offers high wavelength channel counts and ultrashort pulses that will benefit future large-scale high capacity silicon photonic integrated circuits. Here, we demonstrate two-section quantum dot (QD) MLLs that are directly grown on a complementary metal–oxide–semiconductor compatible on-axis (001) silicon substrate by employing molecular beam epitaxy. The lasers, incorporating five layers of InAs QDs, operate in the O-band wavelength range with a pulse repetition rate around 9 GHz. A pulsewidth reduction of 48% of the narrowest achievable pulse from each QD MLL is obtained when the saturable absorber (SA) section length ratio is increased from 8% to 23%. The device with the longest SA section exhibits a more than 50 dB fundamental RF peak signal to noise floor ratio with 1.3 ps pulses. *Published by AIP Publishing*. https://doi.org/10.1063/1.5043200

Photonics can help overcome the physical limits of copper wires to transmit data at higher speed and higher capacity. The integration density of photonic components has evolved rapidly to realize more functionalities and process more data on-chip.[1] Compared to the InP platform, integration density in silicon photonics has grown even faster, benefiting from the mature complementary metal–oxide–semiconductor (CMOS) fabrication technology.[2] Various individual components and large scale photonic circuits have been demonstrated. However, the light generation efficiency of silicon is extremely low due to its indirect bandgap.[3] In order to overcome this last but most frustrating limitation, great efforts have been devoted to demonstrate efficient and reliable light sources on Si, either by flip-chip bonding, wafer bonding or direct growth of quantum dots (QDs).[3,4] A directly grown InAs QD active material on silicon appears to be a promising approach, as QDs are less sensitive to the presence of dislocations introduced by the large lattice constant mismatch between the III/V material and the silicon substrate due to their zero-dimensional carrier localization property.[5] Previous reports of direct growth methods on Si are mainly based on the 4–6° offcut Si substrate in order to suppress antiphase domains. Decent laser performance has been achieved.[6,7] However, CMOS incompatibility of the offcut Si substrate compromises its commercial viability. Recently, significant progress in substrate migration from offcut Si to CMOS compatible on-axis (001) Si with threading dislocation density (TDD) in GaAs buffer layers down to $\sim 7 \times 10^6\,\mathrm{cm}^{-2}$ has been achieved.[8] Record high performance Fabry-Perot (FP) lasers have been demonstrated on this platform with a low lasing threshold and long device lifetime of more than a million hours.[9] In this work, we further extend the device design library to realize monolithic two-section QD mode locked lasers (MLLs) that are based on this material system, as MLLs are important light sources in generating ultra-wide coherent spectra and ultrashort pulses.

The QD material has long been thought advantageous in realizing MLLs over their counterparts in terms of spectral bandwidth, pulse duration, jitter noise performance, and peak power.[10] The advantages over quantum well (QW) or bulk material stem from QDs unique material property, including an inhomogeneous broadband gain spectrum, ultrafast carrier dynamics, large gain and saturable absorber (SA) saturation energy ratio, enhanced temperature stability (large T_0), low linewidth enhancement factor, and low amplified spontaneous emission level.[10,11] Intensive studies on QD MLLs have been conducted on native substrates, demonstrating superior mode locking performance.[10,12] Recently, several reports using QD as gain material to achieve mode locking operation on silicon have been realized via wafer bonding technology.[13,14] Realization of monolithic direct growth of QD MLL sources on the CMOS compatible Si substrate is the next step. In our previous work, a single section MLL source on Si with a 490 fs pulse duration has been demonstrated.[15] Further understanding of this "magic" mode locking behavior is still under investigation. Here, we report our latest results on monolithic two section Si-based QD MLLs that operate in the O-band with a repetition frequency around 9 GHz. Detailed device design, fabrication, and characterization will be covered.

The QD laser epitaxial growth was completed on an on-axis (001) Si substrate with a 45 nm GaP buffer layer by solid-source molecular beam epitaxy (MBE).[16] Detailed epitaxial layer information is shown in Fig. 1(a). An optimized 3.1 μm thick GaAs buffer layer with a low TDD value of $6 \times 10^6\,\mathrm{cm}^{-2}$ was first grown on the substrate to minimize

[a)]S. Liu and J. C. Norman contributed equally to this work.
[b)]Email: stliu@ece.ucsb.edu

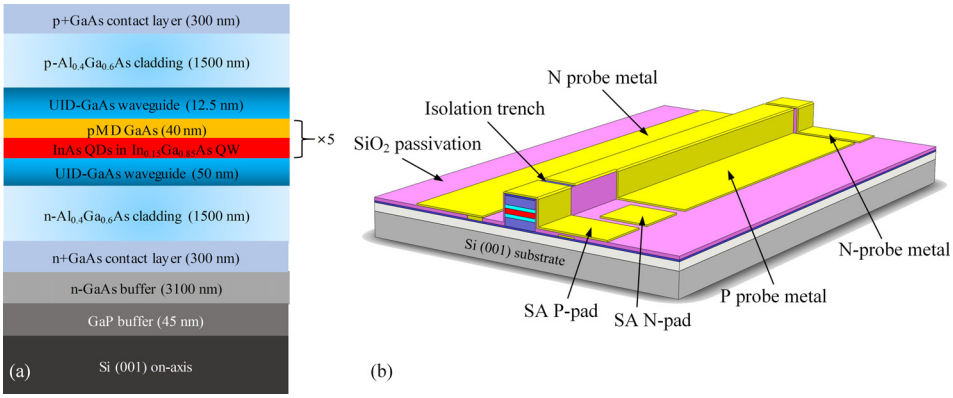

FIG. 1. (a) Schematic diagram of the InAs quantum dot epitaxial layer grown on the GaAs buffer layer on the on-axis (001) Si substrate and (b) schematic diagram of the 9 GHz monolithic quantum dot mode locked laser on silicon (not to scale).

the adverse effect of threading dislocations on laser performance. This was achieved by adopting InGaAs/GaAs strained superlattice dislocation filter layers and a thermal cyclic annealing process.[9] The QD active region consisted of a five-stack InAs/InGaAs dots-in-a-well (DWELL) structure with $5 \times 10^{17}\,\mathrm{cm}^{-2}$ p-modulation doped GaAs spacer layers. The adoption of p-modulation in the active region has been demonstrated to provide more optical gain and better high temperature performance.[6] The dot density is around $6 \times 10^{10}\,\mathrm{cm}^{-2}$ and the photoluminescence full-width at half-maximum is about 30 meV. The top and bottom claddings of this QD laser structure were formed by 1.4 μm thick p- and n-AlGaAs, respectively, with the unintentionally doped GaAs waveguide sandwiching the active region. The whole wafer was then processed into a two-section FP-type MLL configuration as shown in Fig. 1(b) by standard dry etching and deposition techniques. The total length of the laser was designed to be 4500 μm (corresponding to a fundamental repetition frequency of 9 GHz). The SA section length ratio varied from 3% to 23% of the total cavity length. A 3 μm wide deeply-etched ridge waveguide structure down to the n-contact GaAs layer was adopted to facilitate N-metal deposition. Parallel N-metal contacts were placed on both sides of the ridge to ensure current injection uniformity. These were connected via N-probe metal bridges across the ridge, insulated from the p-contact GaAs layer by a SiO_2 insulation layer. A 10 μm long electrical isolation between the SA section and gain section was formed by a second dry etch step to etch away the highly-doped p-contact GaAs layer with an etch depth around 600 nm into the p-cladding layer. The measured isolation resistance is around 18 kΩ. After the fabrication process, the Si substrate was thinned down to ~200 μm to facilitate laser bar cleaving. The laser facets were left as-cleaved.

The fabricated laser bars were tested on a copper heat sink with a stage temperature fixed at 20 °C during the measurement. Four lasers with SA length ratios of 3%, 8%, 13%, and 23% of the total length were investigated. Figure 2 shows the threshold current change as a function of the SA section length ratio (SA section voltage is reverse biased from 0 V to 1.5 V with a step of 0.5 V). The laser thresholds increase as the SA section length increases at different reverse biases as a longer SA section would introduce more absorption loss. Also, the higher the SA section reverse bias of each sample, the higher the absorption loss it will experience, which is enhanced by the reduced absorber recovery time, and the higher the threshold currents it will have. It is interesting to note that the threshold increase is small for shorter SA sections, where the weak quantum confined Stark effect of the QD material plays a role. We also measured the P-I curve of the 23% case sample by sweeping the gain section current upward and downward with fixed SA section voltage biases as shown in the inset of Fig. 2. Clear counter-clockwise hysteresis loops were found. The step-like sudden power rise and fall at threshold is due to the nonlinear saturation effect within the SA section as the intracavity power increases with increased forward biased current, leading to an overall cavity loss decrease. The hysteresis loop width also increases with the increase in the SA section voltage bias, which results from the large difference between the unsaturated and saturated loss of the absorber under higher reverse bias.[17] The series resistances of the samples are around 2.5 Ω. Under the investigated current range, the lasers operated with ground state lasing; no excited state lasing was observed.

Passive mode locking characterization of the QD lasers was done by coupling the optical output signal into an antireflection coated single mode lensed fiber followed by a 45-dB optical isolator. After amplification by an O-band semiconductor optical amplifier (Innolume SOA), the signal was split

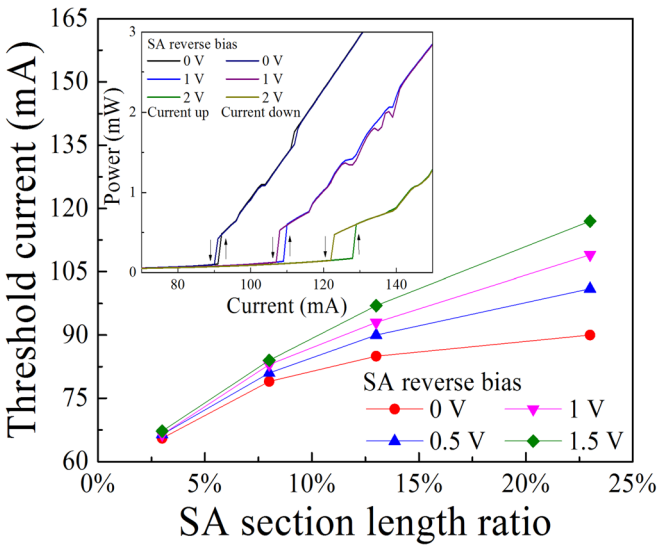

FIG. 2. Threshold current change as a function of SA section length ratio under different SA reverse voltage biases (inset: L-I curve of the QD MLL with 23% SA section length ratio by sweeping the gain section current upward and downward).

and routed to an optical spectrum analyzer (Yokogawa, AQ6370C), a second harmonic generation based background-free autocorrelator (Femtochrome, FM-103MN) for time domain analysis, and an electrical spectrum analyzer (Keysight, N9030A PXA) with a 50 GHz photodiode for RF measurement, respectively. An automated program was developed to record the data simultaneously when sweeping the gain section forward biased current and SA section reversed biased voltage of each laser to characterize the mode locking dynamics.

Passive mode locking regimes of the QD MLLs were delimited by recording operation points with a fundamental frequency signal to noise floor ratio (SNR) larger than 20 dB. The largest mode locking area was found in the QD MLL with 23% SA section length ratio with forward biased current from 100 mA to 160 mA and reverse voltage from 0 V to 2.6 V. Figures 3(a) and 3(b) show the 2D mapping diagram of the fundamental peak SNR and pulsewidth of the QD MLL, respectively. The discrete gray color points within the mode locking area shown in Fig. 3(a) indicate the peak SNR is smaller than 20 dB. As we closely examine the RF spectrum data of these points, the fundamental RF peak is found to be broadened with side peaks compared to other points with SNR larger than 20 dB. Dual RF peaks within 5 MHz were observed in the RF spectrum of one grey data point, indicating two pulse groups competing with each other under this bias condition. Further examination of the optical spectrum shows a shorter wavelength side lobe which begins to rise as the SA reverse bias increases, which causes the instability of the mode locking operation. The reason for this is the absorption peak red shift due to the Stark effect,[10] which alters the threshold modal gain experienced by each wavelength lobe, where the modes that have the lowest threshold gain can become the dominant mode. This lasing mode hopping behavior will perturb the phase locking equilibrium that leads to a low SNR as well as the kink in the L-I curve.[18] Further increasing the SA section reverse bias voltage stabilizes the mode locking operation as the side wavelength lobe becomes the dominant mode, where a high SNR is restored. Figure 3(b) presents the pulsewidth evolution as a function of forward biased current and reverse bias voltage, whose value depends on the interplay between gain and SA section dynamics. In this case, a larger reverse bias voltage gives a narrower pulsewidth at each current point. This is a result of the reduced recovery time of the SA section under higher reverse voltage bias, which narrows the net gain window that the pulse experiences that leads to a total pulsewidth reduction. By comparing the narrowest pulse obtained from each QD MLL device, it is interesting to find that a longer SA section can provide shorter pulses as shown in Fig. 4. A pulsewidth reduction of 48% of the narrowest achievable pulse from each QD MLL can be obtained from 2.5 ps down to 1.3 ps when the SA section length ratio increases from 8% to 23%. A QD MLL with an SA length ratio of 3% demonstrated no mode locking behavior in this investigation. This reducing pulsewidth trend is also found on QD MLLs with native substrates,[10] which is opposite from that of QW MLLs, where lasers with shorter SA section usually generate shorter pulses.[19] The underlying reason can be attributed to the unique properties of the QD material, where an ultralow confinement factor, weak quantum confined Stark effect, and low absorber saturation energy play a role,[20] leading to a different device design methodology between QW and QD material for narrow pulse generation.

The narrowest pulse obtained under this research is shown in Fig. 5(a) from the QD MLL with an SA length ratio of 23% under $I_{gain} = 146$ mA and $V_{SA} = -2.6$ V. The autocorrelation trace is well fit with a hyperbolic secant squared pulse shape with a pulsewidth of 1.3 ps. The corresponding optical spectrum is shown in the inset of Fig. 5(a) with a full width half maximum value around 3.56 nm, which gives a time-bandwidth product (TBP) of 0.81. This somewhat large TBP value indicates a small amount of chirping exists within the pulse, which is normal for long all-active devices. Integrated or external grating pair compression could be introduced to compensate for the dispersion. >130 wavelength lines within 10 dB were obtained, which may be used as a comb source for DWDM systems.[13] Figure 5(b) exhibits the RF performance of the QD MLL in a 50 GHz span view. Sharp RF peaks at the fundamental frequency of 9.1 GHz and its higher order harmonics can be clearly seen. The SNR ratio of the fundamental frequency larger than 50 dB indicates the QD MLL is under stable passive mode locking operation. The Voigt function fit RF 3 dB linewidth is around 80 kHz with a 10 ps integrated

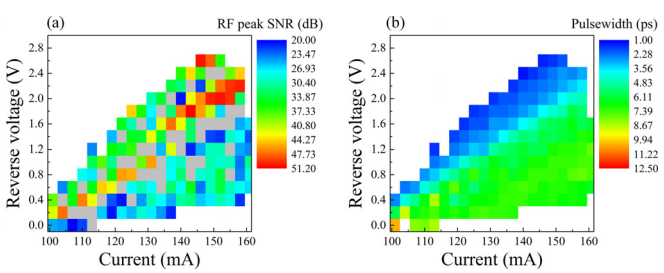

FIG. 3. QD MLL with a SA section length ratio of 23%. (a) Fundamental RF peak signal to noise floor ratio mapping and (b) pulsewidth mapping as a function of gain section current and SA section reverse voltage.

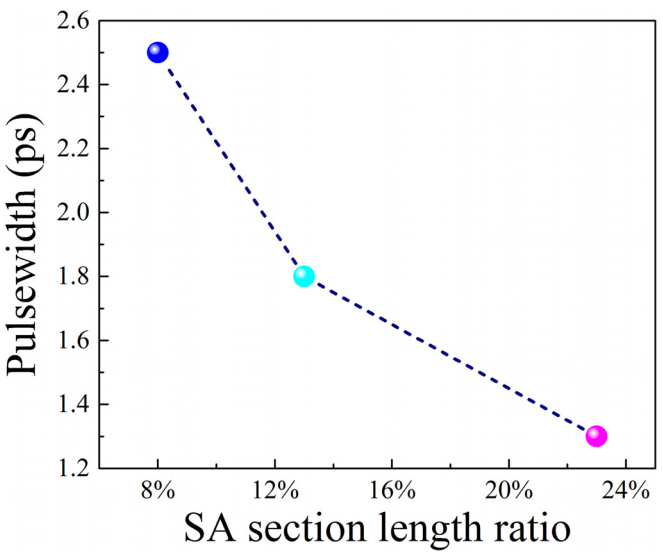

FIG. 4. Narrowest pulsewidth obtained from each QD MLL as a function of the SA section length ratio.

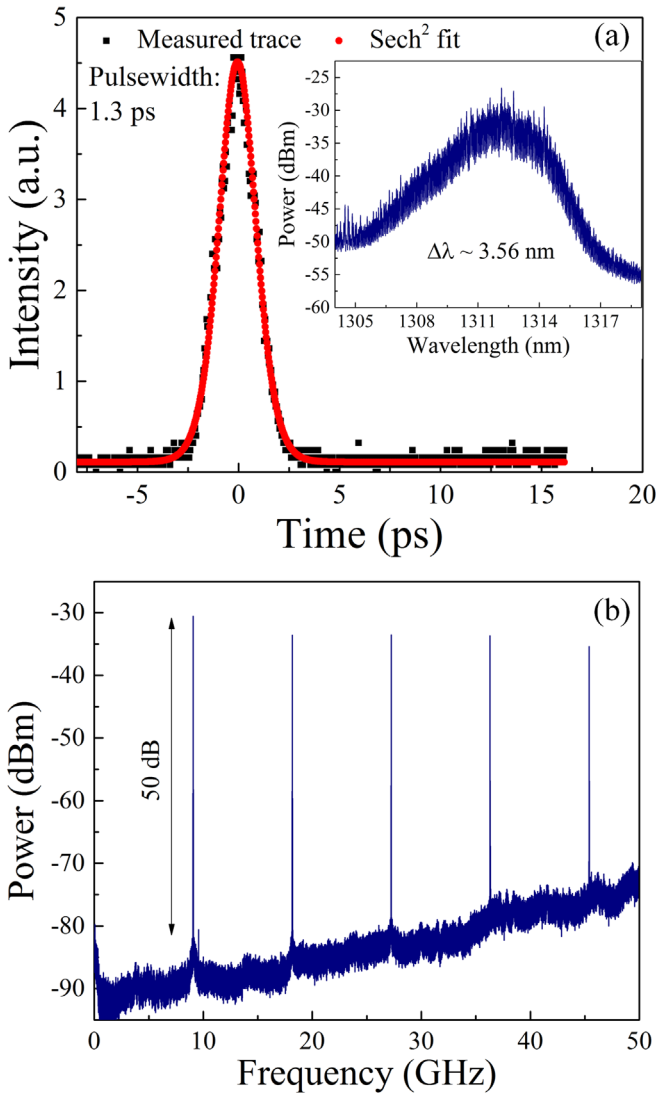

FIG. 5. QD MLL with an SA section length ratio of 23%. (a) Autocorrelation trace with hyperbolic secant squared pulse fitting (inset: corresponding spectrum) and (b) RF spectrum in 50 GHz span view under the narrowest pulsewidth condition (I_{gain} = 146 mA, V_{SA} = −2.6 V, T_{stage} = 20°).

timing jitter by measuring the single sideband phase noise (integration range: 10 kHz–100 MHz).[21]

In conclusion, we have demonstrated the first monolithic two section quantum dot mode locked lasers that are directly grown on on-axis (001) CMOS compatible Si substrates. These lasers operate in the O-band wavelength range with repetition rates around 9 GHz. The QD MLL with the longest SA section length ratio (23%) demonstrates the best performance in terms of the mode locking area and pulsewidth. These achievements represent a major step towards low cost, high wavelength channel count on-chip light sources for large scale silicon photonic integrated circuits.

The work was funded by the Advanced Research Projects Agency-Energy (ARPA-E), U.S. Department of Energy, under Award No. DE-AR00000843. The views and opinions of the authors expressed herein do not necessarily state or reflect those of the United States Government or any agency thereof.

[1]T. Komljenovic, M. Davenport, J. Hulme, A. Y. Liu, C. T. Santis, A. Spott, S. Srinivasan, E. J. Stanton, C. Zhang, and J. E. Bowers, J. Lightwave Technol. **34**, 20 (2016).
[2]M. L. Davenport, S. Skendzic, N. Volet, J. C. Hulme, M. J. R. Heck, and J. E. Bowers, IEEE J. Sel. Top. Quantum Electron. **22**, 3100111 (2016).
[3]D. Liang and J. E. Bowers, Nat. Photonics **4**, 511 (2010).
[4]Z. Wang, A. Abbasi, U. Dave, A. De Groote, S. Kumari, B. Kunert, C. Merckling, M. Pantouvaki, Y. Shi, B. Tian, K. Van Gasse, J. Verbist, R. Wang, W. Xie, J. Zhang, Y. Zhu, J. Bauwelinck, X. Yin, Z. Hens, J. Van Campenhout, B. Kuyken, R. Baets, G. Morthier, D. Van Thourhout, and G. Roelkens, Laser Photonics Rev. **11**, 1700063 (2017).
[5]D. Jung, R. Herrick, J. Norman, K. Turnlund, C. Jan, K. Feng, A. C. Gossard, and J. E. Bowers, Appl. Phys. Lett. **112**, 153507 (2018).
[6]A. Y. Liu, C. Zhang, J. Norman, A. Snyder, D. Lubyshev, J. M. Fastenau, A. W. K. Liu, A. C. Gossard, and J. E. Bowers, Appl. Phys. Lett. **104**, 41104 (2014).
[7]S. Chen, W. Li, J. Wu, Q. Jiang, M. Tang, S. Shutts, S. N. Elliott, A. Sobiesierski, A. J. Seeds, I. Ross, P. M. Smowton, and H. Liu, Nat. Photonics **10**, 307 (2016).
[8]D. Jung, P. G. Callahan, B. Shin, K. Mukherjee, A. C. Gossard, and J. E. Bowers, J. Appl. Phys. **122**, 225703 (2017).
[9]D. Jung, Z. Zhang, J. Norman, R. Herrick, M. J. Kennedy, P. Patel, K. Turnlund, C. Jan, Y. Wan, A. C. Gossard, and J. E. Bowers, ACS Photonics **5**(3), 1094–1100 (2018).
[10]M. G. Thompson, A. R. Rae, M. Xia, R. V. Penty, and I. H. White, IEEE J. Sel. Top. Quantum Electron. **15**, 661 (2009).
[11]J. C. Norman, D. Jung, Y. Wan, and J. E. Bowers, APL Photonics **3**, 030901 (2018).
[12]E. U. Rafailov, M. A. Cataluna, and W. Sibbett, Nat. Photonics **1**, 395 (2007).
[13]G. Kurczveil, M. A. Seyedi, D. Liang, M. Fiorentino, and R. G. Beausoleil, IEEE Photonics Technol. Lett. **30**, 71 (2018).
[14]Z. Wang, M. L. Fanto, J. A. Steidle, A. A. Aboketaf, N. A. Rummage, P. M. Thomas, C.-S. Lee, W. Guo, L. F. Lester, and S. F. Preble, Appl. Phys. Lett. **110**, 141110 (2017).
[15]S. Liu, D. Jung, J. C. Norman, M. J. Kennedy, A. C. Gossard, and J. E. Bowers, Electron. Lett. **54**, 432 (2018).
[16]D. Jung, J. Norman, M. J. Kennedy, C. Shang, B. Shin, Y. Wan, A. C. Gossard, and J. E. Bowers, Appl. Phys. Lett. **111**, 122107 (2017).
[17]X. Huang, A. Stintz, H. Li, A. Rice, G. T. Liu, L. P. Lester, J. Cheng, and M. J. Malloy, IEEE J. Quantum Electron. **37**, 414 (2001).
[18]Y. Li, M. Breivik, C. Y. Feng, B. O. Fimland, and L. F. Lester, IEEE Photonics Technol. Lett. **23**, 1019 (2011).
[19]M. L. Davenport, S. Liu, and J. E. Bowers, Photonics Res. **6**, 468 (2018).
[20]M. G. Thompson, C. Marinelli, Y. Chu, R. L. Sellin, R. V. Penty, L. H. White, M. Van Der Poel, D. Birkedal, J. Hvam, V. M. Ustinov, M. Lammlin, and D. Bimberg, in *2004 IEEE 19th International Semiconductor Laser Conference 2004. Conference Digest* (2004), pp. 53–54.
[21]F. Kéfélian, S. O'Donoghue, M. T. Todaro, J. G. McInerney, and G. Huyet, IEEE Photonics Technol. Lett. **20**, 1405 (2008).